Jour. of the KGS, Vol. 21, No. 2. March 2005, pp. 93~103

Complex Permittivity of Sand at Low Frequency

저주파수 영역에서 측정된 사질토의 유전특성

Oh, Myoung-Hak[1] 오 명 학 Kim, Yong-Sung[2] 김 용 성
Park, Jun-Boum[3] 박 준 범 Yoon, Hyun-Suk[4] 윤 현 석

요 지

본 연구에서는 저주파수 영역에서 유전상수 측정시 발생할 수 있는 왜곡효과를 규명하고, 함수비에 따른 사질토의 유전상수 변화를 실수부와 허수부를 구분하여 조사하였다. 축전기 형태의 셀에서 유전상수를 측정하는 경우 100kHz 이하의 주파수 영역에서 전극분극효과에 의하여 실제 매질의 유전상수보다 크게 측정되었기 때문에 전극분극효과에 의한 영향을 배제하기 위해서는 100kHz 이상의 주파수에서 유전상수가 평가되어야 하는 것으로 판단되었다. 함수비에 따른 사질토의 유전상수를 평가한 결과 체적함수비 증가에 따라 연속적인 증가경향을 나타내었다. 이는 유전상수 실수부의 경우에는 사질토에서 발생하는 분극이 단위체적당 쌍극자 모멘트에 비례하기 때문이며, 유전상수 허수부의 경우에는 함수비 증가에 따른 전도손실량이 증가하기 때문이다. 그러나 유전상수 실수부에서의 체적함수비에 따른 증가경향은 공간전하분극의 영향이 크지 않은 1MHz 이상의 주파수 영역에서 유효한 것으로 나타났다.

Abstract

This study was performed to identify the presence of measurement distortions such as electrode polarization and to investigate the influence of soil water content on complex permittivity at low frequency. In low frequency measurement using two-terminal electrode system, electrode polarization effect was observed at frequencies less than approximately 100 kHz. The analysis for real permittivity should be performed at frequencies above 100 kHz in order to exclude electrode polarization effect in the analysis of real permittivity at low frequency measurements. For a given soil, both of real and effective imaginary permittivity of wet soil increased continuously with volumetric water content. This is evidenced by the facts that the real permittivity is proportional to the number of dipole moments per unit volume and effective imaginary permittivity is affected by the conduction due to water. However, proportional relation between real permittivity and volumetric water content is valid at upper MHz frequencies.

Keywords : Complex permittivity, Electrode polarization, Spatial polarization, Volumetric water content

1. Introduction

Measurement of soil water content is an essential process in any geotechnical and environmental site investigation. Soil water content as a geotechnical parameter is used to evaluate the performance of

1 Member, Post. Doc., Research Institute of Energy and Resources, Seoul National Univ. (omyhak2@snu.ac.kr)
2 Member, Graduate Student, School of Civil, Urban & Geosystem Eng., Seoul National Univ.
3 Member, Associate Prof., School of Civil, Urban & Geosystem Eng., Seoul National Univ.
4 Member, Post. Doc., Geotechnical Engrg. Research Dept., Korea Institute of Construction Technology (KICT)

geotechnical structures such as pavements, foundations, earth dams and retaining walls. In environmental engineering, water content is used in the evaluation of contaminant transport within the vadose zone. Water content may be measured indirectly by determining the dielectric properties of soil. The dielectric properties of a medium describe the response of that medium to an alternating electric field. These properties are conventionally represented by a complex permittivity. Monitoring of soil water content by measuring the dielectric properties is advantageous, as this is fast, with little data processing required to obtain accurate and repeatable results (Rinaldi and Cuestas, 2002). The dielectric properties of soils have been studied in the last decades. The main goals of these studies were directed to the identification of variables that control the dielectric properties of soil in the higher frequencies above a few hundreds MHz. However, few applications of dielectric properties at low frequencies were found in geotechnical engineering. Low frequency measurements turn into an advantage in the following aspects: (1) in-situ testing and monitoring can be performed with little influence of cable impedance; (2) low frequency test devices are comparatively less expensive; and (3) laboratory tests can be performed with very simple capacitive cells (Rinaldi and Redolfi, 1996). The main purposes of this study are to identify the presence of measurement distortions such as electrode polarization and to investigate the influence of soil water content on complex permittivity at low frequency. In this study, alternating current (AC) measurements were performed at frequency ranges between 100 Hz and 12 MHz.

2. Basic Theory of Complex Permittivity

When electric field is applied to a medium, some charges are bound, yet these positive and negative charges can move locally relative to each other in the presence of an electric field, resulting in a polarized medium. This polarizability is represented by the permittivity of a medium. In other words, permittivity is a measure of the extent to which the electrical charge distribution in a material can be polarized by the application of an electric field. To understand permittivity, a basic understanding of capacitance theory is beneficial. Capacitance is the property of a system which permits the storage of electrically separated charges when potential differences exist in a material (ASTM D150 (1994)). Capacitance (C) is defined as the ability of two electrodes to store a charge (Q) when a potential (V) is applied across them. The capacitance is found by Equation (1):

$$C = \frac{Q}{V} = \varepsilon \frac{A}{d} \tag{1}$$

where Q is the charge held on the plates, A is the area of the capacitor, d is the separation between the parallel-plate electrodes and ε is the permittivity of material.

When a capacitor is connected to a sinusoidal voltage source given by Equation (2), the charging current (I_c) in ideal capacitor is expressed as Equation (3):

$$V = V_0 e^{i\omega t} = V_0(\cos\omega t + i\sin\omega t) \tag{2}$$

$$I_c = \frac{dQ}{dt} = \frac{d(CV)}{dt} = C\frac{d(V_0 e^{i\omega t})}{dt} = i\omega C V_0 e^{i\omega t} = i\omega CV \tag{3}$$

where V_0 is voltage amplitude, ω is angular frequency ($=2\pi f$), f is frequency, t is time and i represents imaginary component. The charging current leads the voltage by a temporal phase angle of 90° as shown in Figure 1.

However, in real circumstances, there appears to be a loss current component (I_l) in phase with the voltage in addition to the charging current component as shown in Equation (4).

$$I_l = GV \tag{4}$$

where G represents the dielectric conductance of the material.

The total current traversing the capacitor is inclined by a phase angle (or power factor angle) θ ($< 90°$) against the applied voltage, that is, by a loss angle (or phase defect angle) δ against the +i-axis as shown in Figure 2 (b).

The electrical behavior of a real material is similar to that of a capacitor paralleled by a resistor (RC circuit) as shown in Figure 2 (a). However, the frequency response of RC circuit may not exactly agree with the observed material behavior, because the conductance term in RC

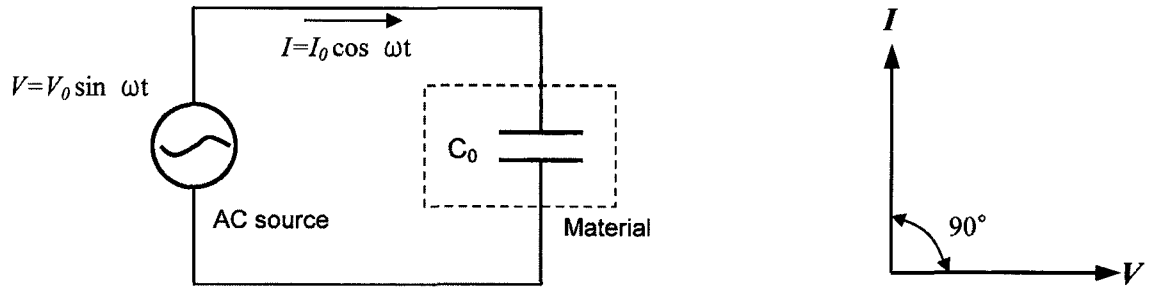

(a) Equivalent circuit (b) current-voltage relation

Fig. 1. Schematic diagram of ideal capacitor

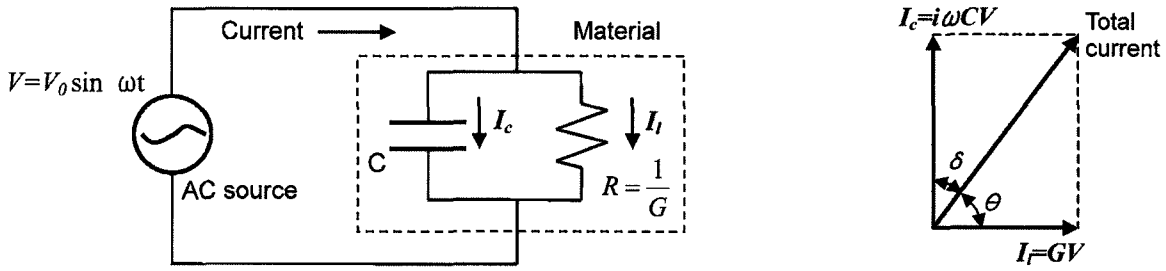

(a) Equivalent circuit (b) total current with loss

Fig. 2. Schematic diagram of real capacitor

circuit is unable to represent energy dissipation loss, for example polarization loss, other than the loss due to migration of charge carrier.

The partially out-of-phase response of real material due to the existence of a loss current in addition to a charging current can be well described by the introduction of complex permittivity (ε*) as shown in Equation (5). And the relative complex permittivity, which is normalized with respect to the permittivity of free space, can be represented by Equation (6) (von Hippel 1954; Shang et al. 1999; Santamarina 2001).

$$\varepsilon^* = \varepsilon' - i\varepsilon'' \tag{5}$$

$$\kappa^* = \frac{\varepsilon^*}{\varepsilon_0} = \kappa' - i\kappa'' \tag{6}$$

In common usage, the word "relative" is frequently dropped (ASTM D150). In this paper, "relative permittivity" is hereafter abbreviated as "permittivity".

The real part of complex permittivity is commonly called permittivity or dielectric constant of material and represents the capacitive behavior or polarizability of the material. On the other hand, the imaginary part is called the loss factor and represents the energy losses due to polarization (Carrier and Soga, 1997; Kaya and Fang, 1997; Shang et al., 2000).

The loss factor, imaginary part of permittivity, is related to the conductivity and frequency by Schwan (1957) and Mitchell and Arulanandan (1968) as

$$\kappa'' = \frac{\sigma_{AC} - \sigma_{DC}}{\omega\varepsilon_0} = \frac{\sigma_{AC} - \sigma_{DC}}{2\pi f\varepsilon_0} \tag{7}$$

in which σ_{AC} is the conductivity at a particular frequency, f, and σ_{DC} is the zero-frequency conductivity.

The σ_{DC} is a real quantity without an out-of-phase component. The out-of-phase component of the permittivity, κ'', is in-phase with the conductivity. Therefore, losses due to polarization and conduction are measured together. The measured loss factor consists of two components, i.e. the dielectric or polarization loss and the loss due to the conduction. It is often reported as a single parameter as effective imaginary permittivity (or effective loss factor) and can be expressed as Equation (8) (Klein, 1999; Shang et al., 2000; Santamarina, 2001).

$$\kappa''_{eff} = \kappa'' + \frac{\sigma_{DC}}{2\pi f \varepsilon_0} \quad (8)$$

Equation (8) shows that the relative contributions of conduction losses and polarization losses can be separated from the measured loss factor.

3. Test Materials and Method

3.1 Test Materials

Two kinds of soil including silica sand (Jumunjin sand) and local soil were used to investigate the permittivity of soil. Local soil was collected from the vicinity of a dormitory at Seoul National University. The local soil used for experimental study will be termed as 'SNU soil' in this paper. SNU soil is weathered granite soil which is commonly found around the Korean peninsula. The physical properties for the test soils are summarized in Table 1. In this study, tap water was used as the natural pore fluid for the soils.

3.2 Test Method

The capacitor-type acrylic mold was specially designed for measuring the permittivity of specimen. Basically, cell consists of acrylic mold, which is an electrical insulator, and two circular electrodes made of brass. The two brass electrodes of capacitor-type cell are 70 mm in diameter and they are 20 mm apart. The sample was placed between the two electrodes in acrylic mold.

The soils were air dried, sieved through sieve No. 10, and then oven dried at 105℃ over 24 hours. The soils were thoroughly mixed with tap water at different water content and then soil-water mixture was put into the acrylic mold and directly compacted to the designed dry density in the mold. Two-electrode measurement was achieved by connecting the test clip leads of measuring device to two brass disc electrodes.

The measurements were achieved using Hewlett-Packard HP4285A Precision LCR meter (Hewlett-Packard, USA) in the range of 75 kHz to 12 MHz and Agilent 4263B LCR meter (Agilent Technologies Japan, Ltd.) in the range of 100 Hz to 1 MHz. Both devices allow for the measurement of capacitance and resistance of material. In order to measure the electrical properties under the low frequency electric field, electrodes of capacitor-type cell are connected to a bridge-type measuring system. Kelvin clip leads (Agilent 16089A) was used to connect the cell to the measuring device. Both electrodes act as current and potential terminals: high current H_c, high potential H_p, low current L_c, and low potential L_p connectors. The configuration of two-terminal electrode system for low frequency measurements is shown in Figure 3. The electrical properties of specimens are determined by measuring the potential difference between the H_p and L_p terminals, and the applied current across the H_c and L_c electrodes. A sinusoidal excitation is imposed and measurements are repeated at different frequencies. Measurements were duplicated at all frequencies providing measuring devices and then each two measured values for capacitance and resistance were averaged to be used for data analysis, only when their deviation lied within 5% ranges.

Table 1. Index and compaction properties of the test soils

	Jumunjin sand	SNU soil
Specific gravity	2.64	2.60
Plasticity Index	NP[1)]	NP[1)]
Coefficient of gradation	1.0	1.4
Uniformity gradation	1.5	8.4
USCS	SP	SW
Percentage passing sieve No.200 (<0.075 mm)	0%	7.6%
Compaction characteristics	$\gamma_{d(max)}$ = 16.3 kN/m^3 $\gamma_{d(min)}$ = 13.0 kN/m^3	$\gamma_{d(max)}$ = 19.1 kN/m^3 w_{opt} = 11.5%

[1)] NP : Non-plastic

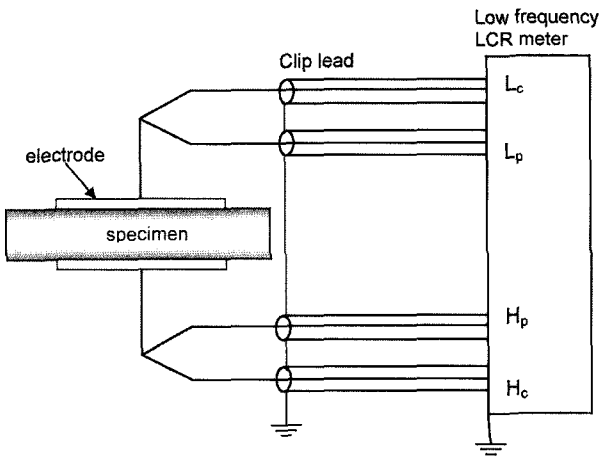

Fig. 3. Two-terminal electrode system for low frequency measurements

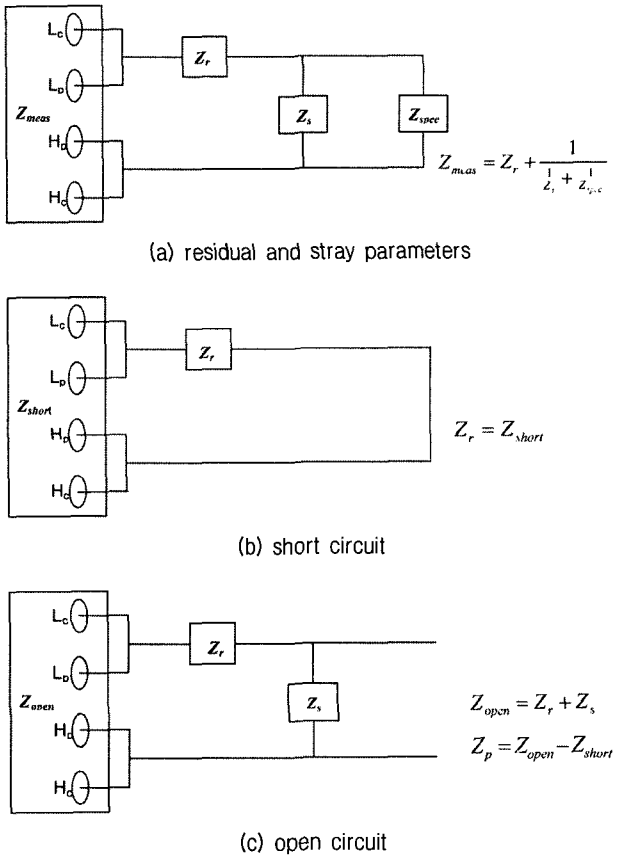

Fig. 4. Equivalent circuit of open and short calibration(modified after Agilent Technologies, 2000; Santamarina, 2001)

4. Calibration and Data Interpretation

4.1 Residual Impedance Effect

In low frequency measurement using two-terminal electrode measurement, there are unwanted residual impedances in series and in parallel with the specimen being tested. These are represented by the equivalent circuit shown in Figure 4 (a). To remove the residual impedance effects, calibration measurements were performed in open-circuit and in short-circuit condition. The short-circuit condition effectively eliminates the stray impedance in parallel, therefore, the measurement Z_{short} determines the residual impedance Z_r in series with the specimen, such as in the test leads. The open-circuit impedance Z_{open} combines the residual and stray impedances in series Z_r and parallel Z_s. The impedance of the specimen Z_{spec} is computed from the measured impedance Z_{meas}, the short-circuit impedance Z_{short} and the open-circuit impedance Z_{open}, as shown in Figure 4.

4.2 Edge Capacitance Effect

In two-terminal measurements, the flow of the electric field in an actual measurement is shown in Figure 5. As shown in Figure 5, edge capacitance or fringe capacitance is formed on the edges of the electrodes and consequently the measured capacitance is larger than the capacitance of the material. When the two electrodes have equal

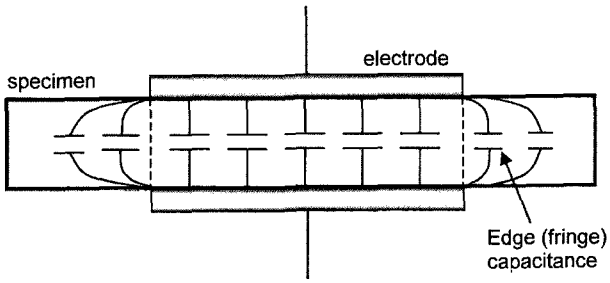

Fig. 5. Schematic diagram of edge capacitance

diameter and are smaller than the specimen, the edge capacitance can be computed as Equation (9) (ASTM D150 (1994)).

$$C_e = (0.0019\kappa' - 0.00252\ln d + 0.0068)p_e \quad (9)$$

$$p_e = \pi(r+d) \quad (10)$$

where, C_e is the edge capacitance [pF] and p_e is the modified perimeter of the electrode plate [mm] where, r is the radius of circular electrode.

The true capacitance value (C_t) can be calculated by subtracting the edge capacitance from the measured capa-

citance (C_m) as Equation (11).

$$C_t = C_m - C_e \tag{11}$$

Therefore, real and effective imaginary permittivity was obtained from following Equations.

$$\kappa' = \frac{C_t}{C_0} = \frac{C_m - C_e}{\varepsilon_0 \times \frac{A}{d}} \tag{12}$$

$$\kappa_{eff}'' = \kappa'' + \frac{\sigma_{DC}}{\varepsilon_0 \omega} = \frac{\sigma_{AC} - \sigma_{DC}}{\varepsilon_0 \omega} + \frac{\sigma_{DC}}{\varepsilon_0 \omega} = \frac{\sigma_{AC}}{2\pi f} \tag{13}$$

The calculated permittivity in capacitor-type acrylic mold was finally calibrated with air, carbon tetrachloride (CCl_4), methanol and deionized water at all measuring frequencies. The real permittivities of them at 20℃ are constant of 1, 2.17, 31 and 79, respectively, at the frequency range used in this study (von Hippel 1954). However, the measured values at 100 Hz were omitted in the analysis of this paper since the measuring device showed a tendency of displaying erratic capacitance values at this frequency.

5. Results and Analysis

5.1 Electrode Polarization Effect

The current in the electrodes, cables, and in the measurement system involves electron flow, while the current in the wet soils is ionic in nature. Given the incompatibility among charges, charge accumulation occurs at the electrode-specimen interface. This effect is called electrode polarization, and it is frequently observed in the low frequency measurement using two-terminal electrode systems. Electrode polarization causes measured real permittivity values to increase as frequency decreases as shown in Figure 6. The real permittivity increased because electrode polarization effect is not representative of material properties (Santamarina, 2001).

Figure 7 shows two-terminal electrode measurements data for deionized water, tap water and aqueous aluminum solutions with varying conductivities. Electrode polarization effects, which cause measured real permittivity values to increase as frequency decreases, were observed at lower frequencies. The minimum frequency at which electrode polarization does not significantly affect the real permittivity measurements is known as the limiting lower frequency. The limiting lower frequency is proportional to the conductivity of material, therefore highly conductive specimens are affected by electrode polarization to higher than low conductivity materials. The range where electrode polarization effects are suspected is denoted on the real permittivity data as shown in Figure 7. It is apparent that values of permittivity at frequencies less than approximately between 10 kHz and 100 kHz are affected by electrode polarization. As shown in Figure 7, it could be estimated that the limiting lower frequency is lower than about 50 kHz.

Some methods have been suggested to eliminate or

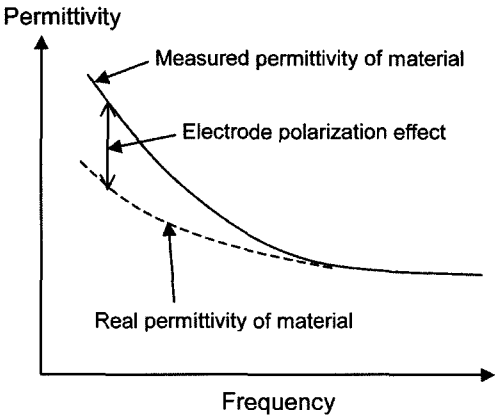

Fig. 6. Resultant effects on measured real permittivity of sample (modified after Carrier and Soga, 1998)

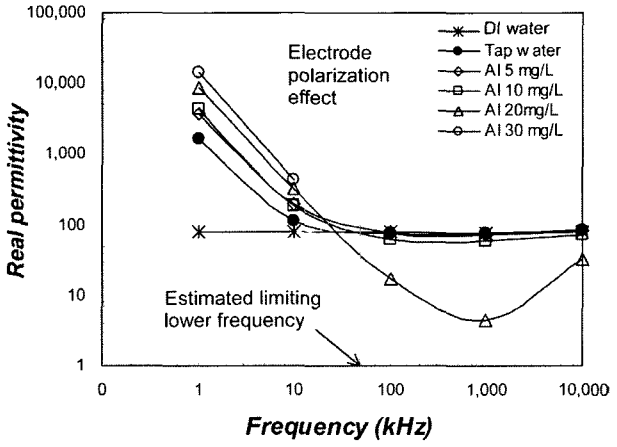

Fig. 7. Spectral response and electrode polarization effect in real permittivity of solution

minimize electrode polarization effects: reversible electrodes (Scott et al., 1967), measurements at two different specimen lengths (Hill et al., 1969), an insulating layer method (Gross and McGehee, 1988), and substitution techniques (Hill et al., 1969). However, based on the analysis of these methods using equivalent circuit models, Santamarina (2001) addressed that these alternatives are mostly ineffective and unreliable because they contribute significant uncertainty to the results. Accurate and effective experimental method for eliminating electrode polarization has not yet been proposed since it is difficult to evaluate the electrode polarization effect quantitatively. Therefore, in this study, the analysis for real permittivity was performed at frequencies above 75 kHz in order to exclude electrode polarization effect in the analysis of real permittivity at low frequency measurements.

5.2 Spectral Response with Frequency

Pure and homogeneous materials consisting of single component have almost certain constant permittivity values at frequencies below approximately 1 GHz. Its values are identical to the summation of three types of polarization mechanisms such as electronic, ionic and orientational polarization. Table 2 shows the real permittivity of some materials. The measured values for selected materials are identical to the reference values with the deviation within 1%. As shown in Table 2, the real permittivity values of given materials are not influenced by frequencies used in this study.

However, the permittivity of soil-water mixtures is influenced by the frequency of the applied electric field. Figures 8 and 9 show the spectral response with frequency of real and effective imaginary permittivity and AC conductivity for the Jumunjin sand and the SNU soil at constant dry unit weight, respectively. For comparison, data for tap water used in this study are also included.

The real and effective imaginary permittivity of soil had a tendency to decrease with increasing frequency, known as relaxation behavior that is similar to the reported permittivity behaviors in the literature (Mitchell and Arulanandan, 1968; Campbell, 1990; Santamarina and Fam, 1997; Klein and Santamarina, 1997). The decreases in real permittivity with frequency suggest a relaxation extending across the kHz region, up to almost 1 MHz for the Jumunjin sand and 10 MHz for the SNU soil. The relaxation across the measuring frequencies is primarily due to spatial polarization producing charge accumulation at interfaces between different phases. Spatial polarization in soil is developed in the interface between pore fluid and soil particles due to ionic migration.

The effective imaginary permittivity (Figures 8 (b) and 9 (b)) and AC conductivity spectra (Figures 8 (c) and 9 (c)) show that the effect of electric conduction is dominant for the total energy losses at frequencies used in this study, and the contribution of polarization losses are not considerable. Rinaldi and Francisca (1999) addressed that the conductivity has a major influence on the effective imaginary permittivity based on the analysis of the contribution of conductivity and polar loss of water molecules in the impedance plane. The linear decrease in effective imaginary permittivity with increasing on the log-log scale signifies that losses in wet soils are dominated by electric conduction. In addition, AC conduc-

Table 2. Real permittivity values of selected materials

Materials		Real permittivity measured in this study				Reference values
		10 kHz	100 kHz	1 MHz	10 MHz	
Deionized water		79.2	78.4	78.0	79.2	79 [1)]
Carbon tetrachloride		2.23	2.26	2.27	2.19	2.17 [1)]
Methanol		30.5	30.8	31.6	31.6	31 [1)]
Dry soil	Jumunjin sand	4.06	3.75	3.52	2.77	3-5 [2)]
	SNU soil	4.66	4.27	3.92	3.00	

[1)] source: von Hippel, (1954)
[2)] source: von Hippel, (1954); Selig and Mansukhani, (1975)

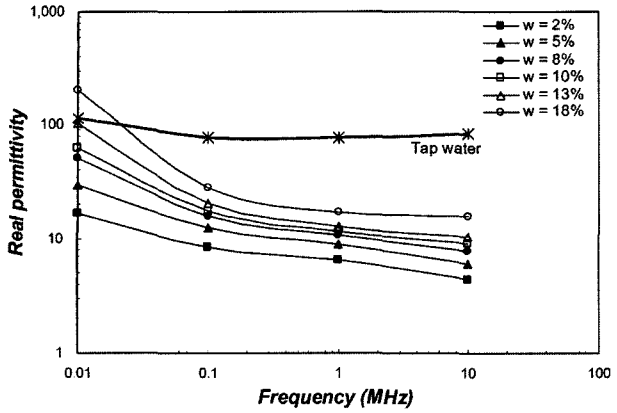

(a) real permittivity

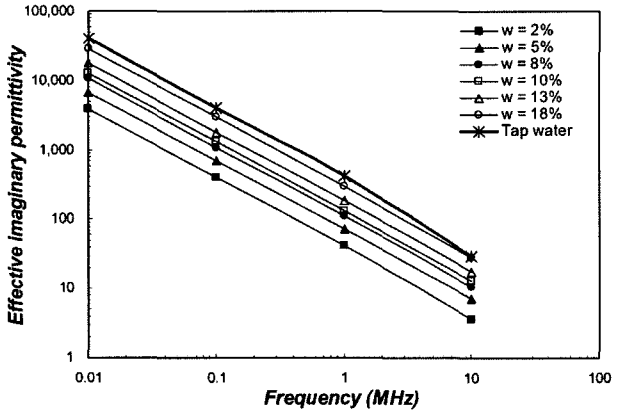

(b) effective imaginary permittivity

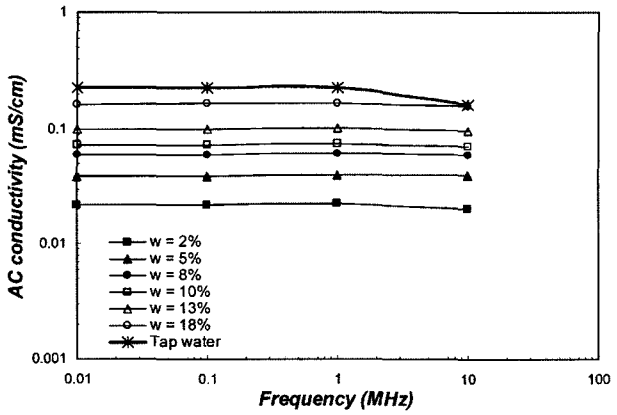

(c) AC conductivity

Fig. 8. Spectral responses with measuring frequency of complex permittivity and AC conductivity for the Jumunjin sand (γ_d=14.2 kN/m^3)

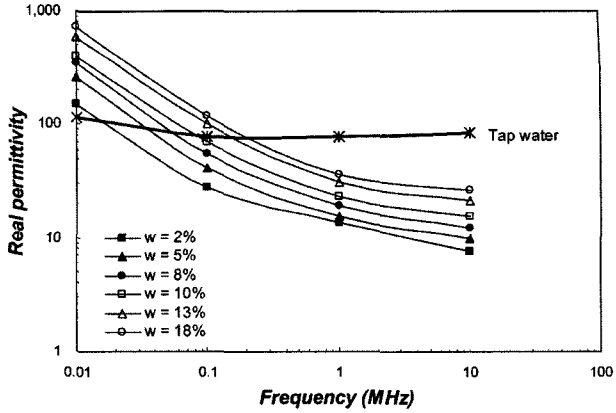

(a) real permittivity

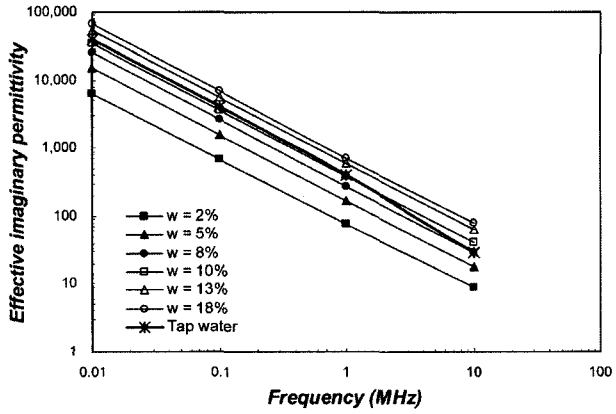

(b) effective imaginary permittivity

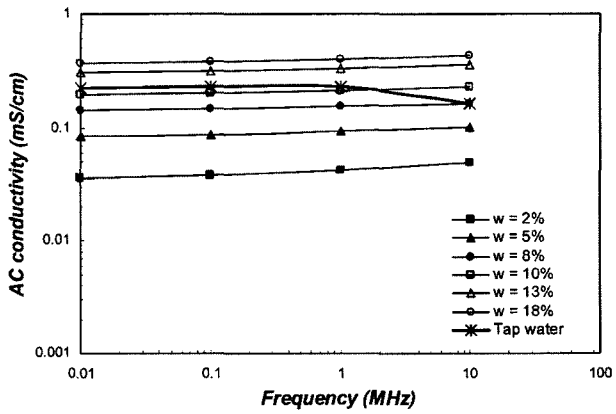

(c) AC conductivity

Fig. 9. Spectral responses with measuring frequency of complex permittivity and AC conductivity for the SNU soil(γ_d=15.7 kN/m^3)

tivity reflects the effect of both direct current (DC) conduction and polarization losses. The variations of AC conductivity with frequency are little and can be negligible as shown in Figures 8 (c) and 9 (c). These results imply that the additional polarization losses besides the conduction losses can be negligible, although the polarization losses are simultaneously developed. Therefore, test results indicate that the energy losses represented by effective imaginary permittivity are mainly due to electric conduction losses.

5.3 Influence of Water Content on Permittivity of Soil

It is reasonable to claim that permittivity is governed by volumetric water content since the permittivity is proportional to the number of dipole moments per unit volume. The volumetric water content is defined as the ratio of the volume of pore water (V_w) to the total volume of soil (V_t). The volumetric water content (θ_v) can be also defined as represented in Equation (14).

$$\theta_v = \frac{V_w}{V_t} = \frac{\gamma_d w}{\gamma_w} \tag{14}$$

where, γ_d is the dry unit weight and w is gravimetric water content, and γ_w is the unit weight of water.

The real and effective imaginary permittivity for the Jumunjin sand and the SNU soil with volumetric water content at three different frequencies, 100 kHz, 1 MHz and 10 MHz, are shown in Figures 10 and 11. In Figures 10 (a) and 11 (a), the real permittivity of soil increased with increasing volumetric water content and decreasing frequency. The increase of volumetric water content means that the number of the permanent electric dipoles such as water molecules which can cause orientational polarization increases and the amount of air in pore decreases. Therefore it is apparent that the real permittivity of soil increased with volumetric water content. In Figures 10 (b) and 11 (b), the effective imaginary permittivity of soil also increased with increasing volumetric water content and decreasing frequency. The increases of effective imaginary permittivity of soils with volumetric

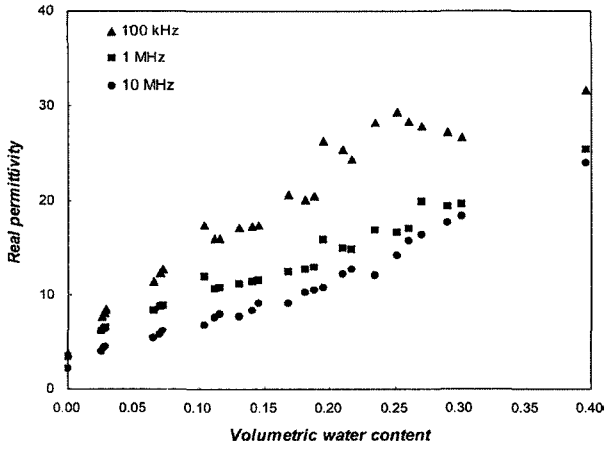

(a) Real permittivity

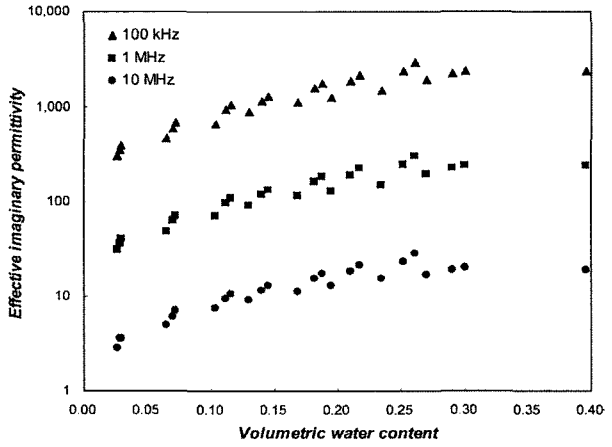

(b) Effective imaginary permittivity

Fig. 10. Relationship between permittivity and volumetric water content for the Jumunjin sand at the frequency of 100 kHz, 1 MHz and 10 MHz

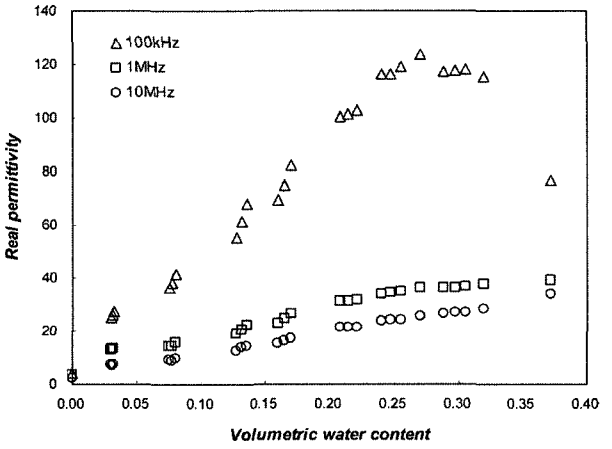

(a) Real permittivity

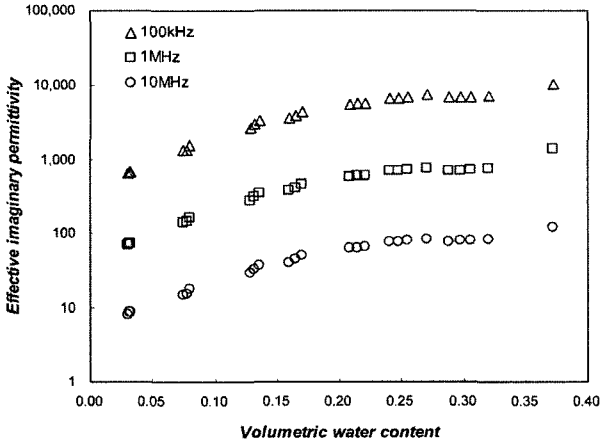

(b) Effective imaginary permittivity

Fig. 11. Relationship between permittivity and volumetric water content for SNU soil at the frequency of 100 kHz, 1 MHz and 10 MHz

water content can be explained by the increase of the conduction loss caused by the increase of connected pores and the number of water molecules.

The increase of real permittivity of soil with measuring frequencies implies that the spatial polarization, which was formed in mixture at low frequencies, was still dominant at 1 MHz. The effect of spatial polarization was more dominant in the SNU soil as shown in Figures 8 and 9. Especially, the real permittivity of the SNU soil at 100 kHz presented in Figure 11 (a) shows that the real permittivity of the soil-water mixture exceeds the permittivity of water and reaches a peak, and then decreased with volumetric water content at higher volumetric water content, but not at high frequencies. Since the spatial polarization was developed at low frequencies, it is apparent that trends of permittivity versus volumetric water content vary in the different frequency bands. Santamarina (2001) addressed that at the lower frequencies, in which the spatial polarization was dominant, the permittivity increased with volumetric water content starting at the value of real permittivity of dry soil, until a peak was reached where the $\kappa'_{mix} > \kappa'_{w}$ and further addition of water causes a decay in permittivity towards the permittivity of water. However, at higher frequencies, the real permittivity was determined by the polarizability of the free water, therefore the real permittivity of the wet soil increased continuously with volumetric water content.

6. Conclusions

The main conclusions derived from the experimental research for complex permittivity of sand at low frequency are summarized as follows.

(1) For a given soil, the complex permittivity of sand was strongly governed by the volumetric water content of soil. Both of real and effective imaginary permittivity of wet soil increased continuously with volumetric water content. This is evidenced by the facts that the real permittivity is proportional to the number of dipole moments per unit volume and effective imaginary permittivity is affected by the conduction due to water. However, proportional relation between real permittivity and volumetric water content is valid at upper MHz frequencies.

(2) The frequency dependent behaviors observed in the real permittivity of soil was the result of spatial polarization due to the charge accumulation at the interfaces between phases. The effect of spatial polarization was magnified at lower frequencies (kHz ranges). The linear decreases in the effective imaginary permittivity of soil in log-log plots indicate that conduction losses were dominant for the total energy losses at the frequencies used in this study.

(3) In low frequency measurement using two-terminal electrode system, electrode polarization effect was observed at frequencies less than approximately between 10 kHz and 100 kHz. However, accurate and effective experimental method for eliminating electrode polarization has not yet been proposed. Future works for quantitative evaluation of electrode polarization are recommended.

Acknowledgement

This work was supported by grant No. R01-2002-000-00136-0 from the Basic Research Program of the Korea Science & Engineering Foundation.

References

1. Agilent Technologies (2000), *Impedance Measurement Handbook*, 2nd Ed., Agilent Technologies Co. Ltd.
2. ASTM D150 (1994), *Standard test methods for AC loss characteristics and permittivity (dielectric constant) of solid electrical insulation*, ASTM D150-94, Philadelphia
3. Campbell, J. E. (1990), "Dielectric properties and influence of conductivity in soils at one to fifty megahertz", *Soil Science Society of American Journal*, Vol.54, pp.332-341
4. Carrier, M. and Soga, K. (1997), "A four terminal measurement system for the investigation of the dielectric properties of clay at low frequencies", *Geoenvironmental Engineering*, Thomas Telford, London, pp.3-10.
5. Gross, G. W. and McGehee, R. M. (1988), "The layered-capacitor method for bridge measurements of conductive dielectrics", *IEEE Transactions on Electrical Insulation*, Vol.23, pp.387-396.
6. Hill, N. E., Vaughan, W. E., Price, A. H., and Davies, M. (1969), *Dielectric properties and molecular behaviour*, Van Nostrand Reinhold Company Ltd., U.K.

7. Kaya, A and Fang, H. Y. (1997), "Identification of contaminated soils by dielectric constant and electrical conductivity", *Journal of Environmental Engineering*, ASCE, Vol.123, No.2, pp.169-177.
8. Klein, K. (1999), "Electromagnetic properties of high specific surface minerals", Ph.D. thesis, Department of Civil Engineering, Georgia Institute of Technology, USA.
9. Klein, K. and Santamarina, J. C. (1997), "Methods for broad-band dielectric permittivity measurements (soil-water mixtures, 5 Hz to 1.3 GHz)", *Geotechnical Testing Journal*, ASTM, Vol.20, No.2, pp.168-178.
10. Mitchell, J. K. and Arulanandan, K. (1968), "Electrical dispersion in relation to soil structure", Journal of the Soil Mechanics and Foundations Division, ASCE, Vol.94, No.SM2, pp.447-471.
11. Rinaldi, V. A. and Cuestas, G. A. (2002), "Ohmic conductivity of a compacted silty clay", *Journal of Geotechnical and Geoenvironmental Engineering*, ASCE, Vol.128, No.10, pp.824-835
12. Rinaldi, V. A. and Francisca, F. M. (1999), "Impedance analysis of soil dielectric dispersion", *Journal of Geotechnical and Geoenvironmental Engineering*, ASCE, Vol.125, No.2, pp.111-121.
13. Rinaldi, V. A. and Redolfi, E. R. (1996), "The dielectric constant of soil-NAPL mixtures at low frequencies (100 Hz - 10 MHz)", *Proceeding of Nonaqueous Phase Liquids (NAPLs) in the Subsurface Environment: Assessment and Remediation*, ASCE, Washington D.C., pp.163-174.
14. Santamarina, J. C. (2001), *Soils and Waves*, John Wiley & Sons.
15. Santamarina, J. C. and Fam, M. (1997), "Dielectric permittivity of soils mixed with organic and inorganic fluids (0.2 GHz to 1.30 GHz)", *Journal of Environmental and Engineering Geophysics*, Vol.2, No.1, pp.37-51.
16. Schwan, H. P. (1957), "Electrical properties of tissues and cell suspensions", *Biological and Medical Physics*, 5.
17. Scott, J. H., Caroll, R. D., and Cunningham, D. R. (1967), "Dielectric constant and electrical conductivity measurements of moist rock: A new laboratory method", *Journal of Geophysical Research*, 72, pp.5101-5115.
18. Selig, E. T. and Mansukhani, S. (1975), "Relationship of soil moisture to the dielectric property", *Journal of the Geotechnical Engineering Division*, ASCE, Vol.101, Vol.GT8, pp.755-770.
19. Shang, J. Q., Rowe, R. K., Umana, J. A., and Scholte, J. W. (1999), "A complex permittivity measurement system for undisturbed/ compacted soils", *Geotechnical Testing Journal*, ASTM, Vol.22, No.2, pp.159-168.
20. Shang, J. Q., Scholte, J. W., and Rowe, R. K. (2000), "Multiple linear regression of complex permittivity of a till at frequency range from 200 MHz to 400 MHz", *Subsurface Sensing Technologies and Applications*, Vol.1, No.3, pp.337-356.
21. von Hippel, A. R. (1954), *Dielectric Materials and Applications*, von Hippel, A. R. ed., The Technology Press of Massachusetts Institute of Technology.

(received on Mar. 7, 2005, accepted on Mar. 28, 2005)